International Research Journal of Engineering and Technology (IRJET) e-ISSN: 2395-0056
Volume: 06 Issue: 08 | Aug 2019 www.irjet.net p-ISSN: 2395-0072

Investigation on Dissimilar Metal Welding of Stainless Steel 316 L and Mild Steel A-2062 Using GTAW

Manish Kumar[1], Anil Punia[2]

[1]*Post graduate student, Department of Mechanical Engineering, Rao Pahlad Singh College of engineering and technology, Mohindergarh, Haryana-123023, India*
[2]*Assistant Professor, Department of Mechanical Engineering, Rao Pahlad Singh College of engineering and technology, Mohindergarh, Haryana-123023, India*

Abstract: *GTAW process can be performed on similar or dissimilar. The two dissimilar metals which need to be joined will have different mechanical properties, thermal properties and microstructures which in will always going to affect welding parameters and quality of weld. When two dissimilar component of machine is undergoing any repair these problems always predominant. The study of mechanical properties of welding of dissimilar is important because welded structure may be installed at highly sensitive and risky place. Problem of formation of inter-metallic compound may arise which affect the weld quality. This Experimental work investigates the technical considerations of dissimilar metal welding between IS2062 Grade C mild steel and 316L stainless steel using the GTAW process. The tensile behavior, micro hardness number study, welding responses (depth of penetration, weld bead width) were also explained. Finite element analysis of dissimilar metal joints are also analyzed and compared with experimental work. The tensile strength of samples ranges 394 MPa to 454 MPa. Micro hardness was slightly more than both base materials. Microstructure analysis is also done for high heat input sample, low heat input sample and highest UTS sample*

Key words: Tungsten inert gas welding, dissimilar metal welding, micro hardness, Depth of penetration, Ultimate tensile strength.

I. INTRODUCTION

Joining of dissimilar metals is having great use in power plants, electronic parts industries, nuclear reactors, petrochemical/chemical industries generally to obtain tailor-made properties into their components with reduction in weight. However welding with high efficiency of dissimilar metals is having a major challenge due to difference in properties of the materials to be joined under same welding condition. Difference in thermal properties causes a steep gradient along the weld[1]. A variety of problems come up in dissimilar welding like cracking, large weld residual stresses, migration of atoms during welding causing stress concentration on one side of the weld, 1zcompressive and tensile thermal stresses, stress corrosion cracking, etc. Now before discussing these problems coming up during dissimilar welding, the passages coming below throw some light on some of the causes of these[3] problems. **Jiang and Guan** studied the thermal stress and residual stress in dissimilar steels. They suggested that large residual stresses are induced by welding in the weld metal and heat affected zone (HAZ), which superimpose and increase the thermal stress. They studied the thermal stress and residual stress in dissimilar steels. They suggested that large residual stresses are induced by welding in the weld metal and heat affected zone (HAZ), which superimpose and increase the thermal stress[1]. **Chengwu et al**. did work on weld interface microstructure and mechanical properties of copper-steel dissimilar welding, the microstructure near the interface between Cu plate and the intermixing zone was investigated. Their results showed, for the welded joint where dilution ratio is high like of copper, in the transition zone there was numerous filler particles available near the interface with base metal. For low dilution ratio of copper, the transition zone is present near the upper side of the WZ-base metal interface. At the lower side of the interface, the turbulent bursting behavior in the welding pool led to the penetration of liquid metal into Cu. The welded joint with lower dilution ratio of copper in the fusion zone exhibited higher tensile strength[2]. **Gyun Na, Kim and Lim** studied the residual stress and its prediction for dissimilar welds at nuclear plants using Fuzzy Neural network models. The factors that have an impact upon fatigue strength is residual stress, stress concentration, the mechanical properties of the material, and its micro and macro structure. They also stated that residual stress is one of the most important factors but its effect on high-cycle fatigue is of more concern than the other factors[3]. **Khan et al.** studied laser beam welding of dissimilar stainless steels in a fillet joint configuration and during the study metallurgical analysis of the weld interface was

done. Fusion zone microstructures contained a variety of complex austenite ferrite structures. Micro-hardness of FZ was higher than both base metals. **Itoh et al.** got a patent on the joined structure on the dissimilar metallic materials. This invention relates generally to a joined structure of dissimilar metallic materials having different characteristics[4]. **Delphin, Sattari-Far and Brickstad** studied the effect of thermal and weld residual stresses on CTOD (Crack Tip Opening Displacement) in elastic-plastic fracture analysis. They stated that structures may fail because of crack growth both in welds and in the heat affected zone (HAZ). The welding process itself induces residual stresses in the weld and HAZ, which contribute to crack growth[5]. **Colegrove et al.** studied the welding process impact on residual stress and distortion. Their work seeks to understand the relationship between heat input, fusion area, measured distortion and the residual stress predicted from a simple numerical model, and the residual stresses is validated with experimental data[6]. In present work Stainless steel 316 L and Mild steel A-2062 is used because of its wide application in Heat Exchangers, Pipelines, Pressure Vessels, Flanges and Fittings. Chemical composition and Mechanical properties are written in Table 1 and Table 2.

Table 1. Chemical composition of 304l stainless steel

Material	C %	Mn %	S%	P%	ni	Mo	Si
Mild steel IS-2062	0.23	1.5	0.05	0.05	0.00	0.00	0.04
Stainless steel 316 L	0.03	2.0	0.75	0.045	10.00	2.00	0.75

Table 2. mechanical property of stainless steel aisi 304l

Material	UTS (MPa)	Y.S. (MPa)	Vickers's hardness Number	EI. %
Mild steel IS-2062	410	250	180	23
Stainless steel 316 L	485	170	220	40

2. METHODOLOGY

2.1 Process parameters and their range: In the present investigation only three major parameters viz. welding speed, welding current and gas pressure have been varied with four levels for different experimental runs by keeping other parameters constant.

Table 3. Process parameters for TIG welding

Parameters	Units	Level 1	Level 2	Level 3	Level 4
Welding speed (S)	m/min	0.25	0.3	0.35	0.40
Welding current (I)	Amp	120	140	160	180
Gas pressure (G)	Kg/cm^2	10	15	20	25

2.2. Design of experiment: Design of Experiment is done as per Taguchi L16 array in for three different parameter level. Total 16 samples were prepared for various parameter ranges as given in table 4.

Table 4. Design of experiment as per Taguchi's method l16 orthogonal array for welding with flux

S. NO.	Level of parameter		
	Current (I)	Welding speed(S)	Gas flow rate(G)
1	1	1	1
2	1	2	2
3	1	3	3
4	1	4	4
5	2	1	2
6	2	2	1
7	2	3	4
8	2	4	3
9	3	1	3
10	3	2	4
11	3	3	1
12	3	4	2
13	4	1	4
14	4	2	3
15	4	3	2
16	4	4	1

2.3. Sample preparation: With the help of power saw both types of plates were cut in the dimension of 50mm×25mm×6mm in presence of coolant. To make every edge at right angle, machining with shaper was done. Before welding the specimens were mechanically cleaned by filing followed by cleaning by emery paper.

3. RESULT AND DISCUSSION

3.1. Tensile test: Tensile testing was carried out using Universal Testing Machine of 400 KN capacity and the geometry of the test specimen is as shown in Fig. 1. Specimens were prepared as per ESTM E8. As per tensile test result, the UTS of welding joints vary from 394 to 457 MPa depending upon the welding conditions. All the specimens broke in the weld region and percentage of elongation measured across the weldment using an extensometer show ductility ranging from 5.77% to 6.6%.

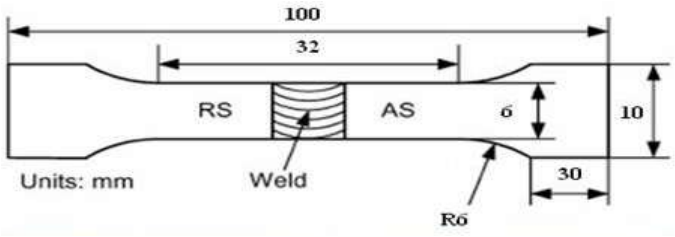

Figure 1. Tensile test specimens as per ASTM E8

The value of peak stress is considered as ultimate tensile strength of the joint as all specimens were found to break from joint[10]. The maximum UTS was obtained for sample no 8. After welding, the cooling was done in air that may have annealed the samples because of which strength is increased.

Table 5. Tensile test values of dissimilar metal welded joints (AISI 316L & IS 2062)

Sample Number	Ultimate tensile strength (MPa)	Percentage elongation
1	399	5.853172
2	394	5.779824
3	420	6.161233
4	425	6.234581
5	399	5.853172
6	406	5.955859
7	430	6.30793
8	454	6.66
9	450	6.601322
10	430	6.30793
11	420	6.161233
12	430	6.30793
13	410	6.014537
14	395	5.794493
15	399	5.853172
16	409	5.999868

The stress strain curve for highest UTS (sample 8) and lowest UTS (sample 2) is explained in Fig. 3. The tensile test of the welded specimen results in the strength of joint being above UTS of mild steel and below to UTS of stainless steel. The joint strength is achieved as high as 454. To conclude the brittleness effect the hardness test and microstructure analysis is done for the sample with highest ultimate tensile strength, highest heat input sample and lowest heat input sample.

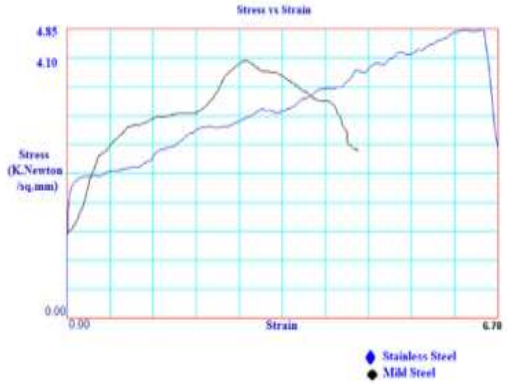

Figure 2. Stress strain curve for Base materials (SS 316 L and MS 2062)

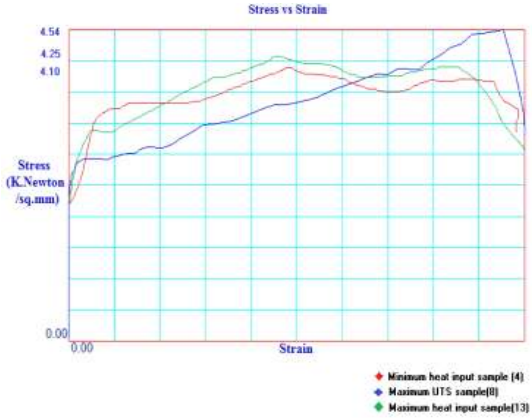

Figure 3. Stress strain curve for minimum heat input, maximum heat input and highest UTS sample

Table 6. Stress strain properties for sample 8 at various load condition and time.

Stress (MPa)	Strain (%)	Force (kN)	Position (mm)	Time (s)
0	0.5	0.00	0	0.109
36.6	1.16	8.78	0.347	21
69	2.45	4.61	0.71	42.8
128	3.64	3.06	1.07	64.5
187	5.256	4.48	1.44	86.3
243	6.45	5.84	1.8	108
289	8.456	6.99	2.16	130
298	10.21	7.15	2.52	152
314	11.2	7.54	2.89	173
328	14.45	8.14	3.25	195
339	15.32	8.39	3.61	265

378	18.45	8.65	3.98	295
398	21.78	9.07	4.34	345
414	22.89	10.29	4.70	375
430	24.98	10.95	5.60	398
439	26.77	11.24	5.98	425
454	29.43	12.39	6.32	455
445	31.23	11.54	6.53	485
430	32.54	11.03	6.78	502
428	33.56	10.65	7.02	532
402	34.15	9.45	7.25	556
385	34.98	9.21	7.45	575
345	35.68	8.71	4.56	586

3.2. Effect on micro hardness, depth of penetration and weld bead width: Micro hardness of the all sample in weld zone as well as heat affected zone was measured in this research work. The average hardness number was calculated for weld zone as well as HAZ as shown in table 7. Hardness number (vicker's) for the weld zone as well as heat affected zone is slightly more than Mild steel AISI 2062 but nearly equal to that of stainless steel[11] 316L as shown in Fig. 4. The depth of penetration, weld bead width is also given for each sample as well as average in table no 7. The average depth of penetration was good to weld the material in single pass in both sides as average penetration was 5.8484. Average weld bead width was also 4.8243. Since average hardness was slightly higher than base materials, to check the brittleness of the samples, microstructure analysis was done which is explained in next section.

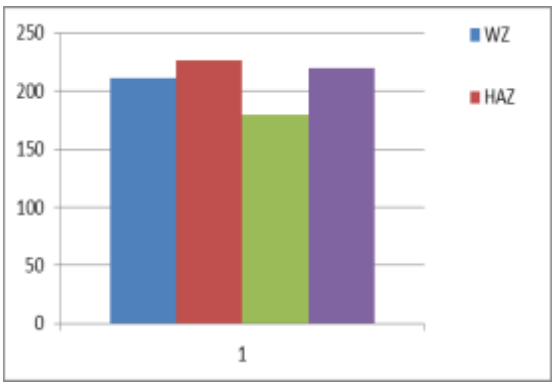

Figure 4. Chart showing hardness comparison of both base metal with welding zone and HAZ

Table 7. Table showing value of welding responses

Experiment no	Depth of penetration (mm)	Bead width (mm)	Hardness of weld zone ($HV_{0.5}$)	Hardness of HAZ ($HV_{0.5}$)
1	5.8087	4.520	269.92	245.1
2	5.3049	2.362	220.63	220.5
3	5.2479	2.086	221.83	234.54
4	5.3107	2.610	257.28	262.4
5	5.8471	4.464	255.69	241.16
6	5.6871	3.280	224.26	221.5
7	5.661	4.731	232.14	240.7
8	5.6516	3.379	212.81	222.7
9	5.2661	6.293	251.97	232.51
10	5.0112	6.714	214.35	216.92
11	5.9658	3.805	203.37	205.43
12	5.8716	5.165	197.57	209.1
13	5.5034	8.354	226.63	231.97
14	5.2521	7.431	201.19	202.5
15	5.2127	6.739	212.27	207.1
16	5.967	5.248	229.96	221.3
average	5.8481	4.824	211.011	225.964

3.3. Microstructure analysis: Microstructure analysis of the sample having highest ultimate tensile strength (sample 8), highest heat input (sample 13) and lowest heat input (sample 8) is done towards both base materials.

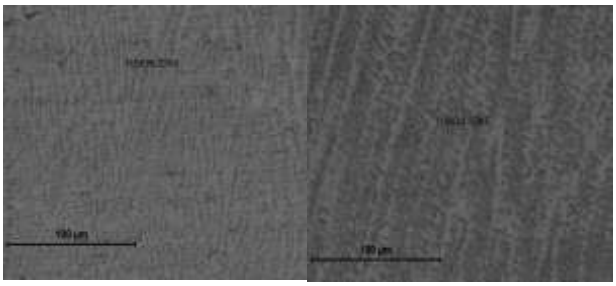

Figure 5. Microstructure of (a) sample 8 (highest UTS) in fusion zone (b) sample 13 (highest heat input) in fusion zone

Fig. 5 explaining the microstructure in fusion zone of sample 8 showing whitish grain which indicates presence of austenite in the zone[11]. It can also be used to verify that brittleness is not increased of the sample 8 in fusion zone.

Similarly for sample 13 the microstructure comes vary similar as shown in Fig 5. Microstructure of all zones towards the stainless steel 316 L (for mentioned samples) is showing presence of coarse grain structure hence forming pearlite and some retained austenite into it[12].

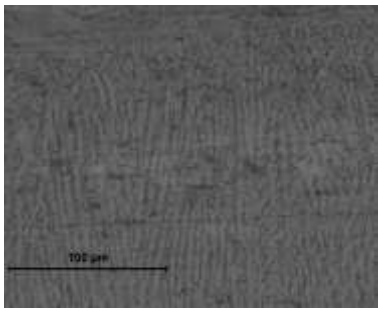

Figure 6. Microstructure of (c) sample 4 (lowest heat input) in fusion zone

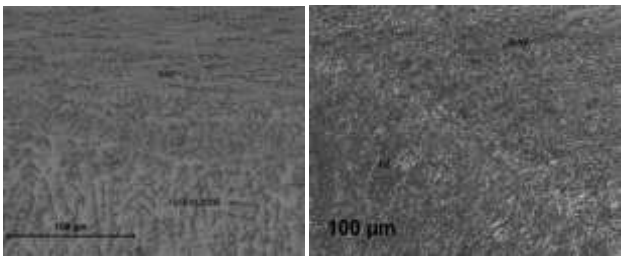

Figure 7. Microstructure of sample 8(Highest UTS) showing WZ and HAZ interface towards (a) SS 316L (b) MS 2062

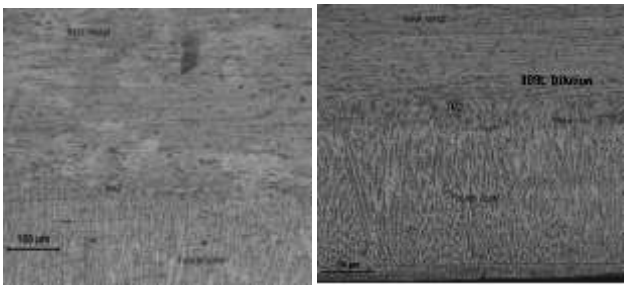

Figure 8. Microstructure of sample 8(Highest UTS) showing (a) base metal and HAZ interface towards SS 316L (b) base metal and HAZ interface towards MS 2062

Towards mild steel zone hardness was little high as compared to stainless steel zone as some sorbitic and martensitic grains found (black portions) which is major cause of slightly hike in hardness[10]. But overall tensile strength and presence of coarse grain makes the welding more valuable[11]. Various zone of the mentioned sample are shown in Fig. 6 to Fig. 8. Dilution of filler rod 309L is seen more towards the HAZ and base metal.

3.4. Element analysis of dissimilar metal joints:

The results are obtained after considering the weld zone simulation. In the first case AISI 309L stainless steel has been taken as the weld filler metal whose properties are taken the same as AISI 316L stainless steel which is one of the parent metals.

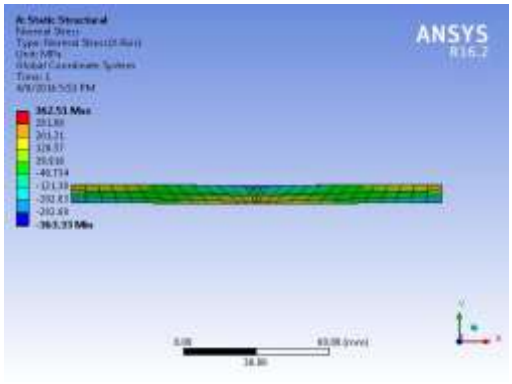

Figure 9. Normal stress contour of Model

So the results inferred from all the stress acted on it. Thermal stress has developed inside the welded part as both of its ends across the weld have been fixed against any kind of motion by setting up in nodal displacement in all directions as zero[2]. This is the boundary conditions used in all areas. The normal stress varies from 362 MPa tensile to 363MPa compressive.

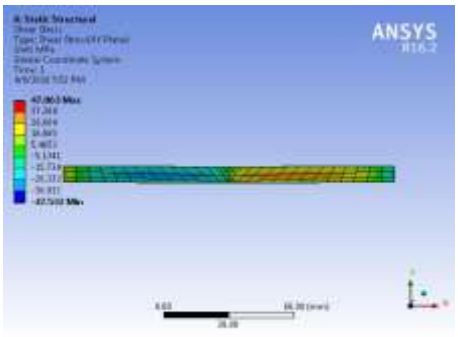

Figure 10. ANSYS model showing shear stress contour of Model

The peak of the tensile stress lies along the centerline of the weld metal. However peak of the compressive stress lies in the weld interface of weld filler metal and IS 2062 mild steel as mentioned in Fig. 9. The shear stress varies from 478 MPa positive to 475 MPa negative.

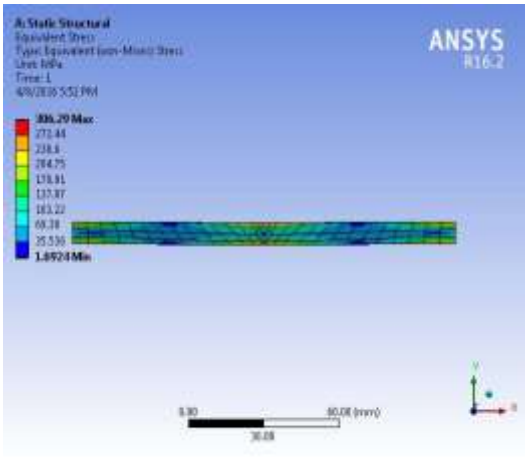

Figure 11. ANSYS model showing von-mises stress.

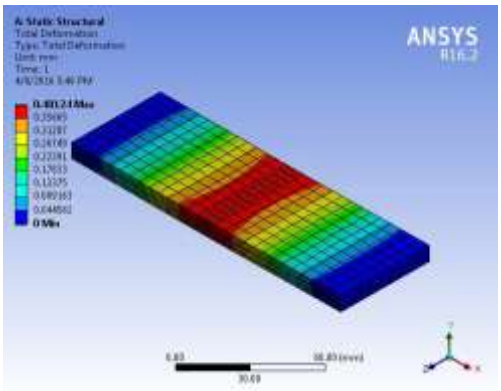

Figure 12. ANSYS model showing total deformation

However peak of the shear stress lies in the weld interface of weld filler metal and 2062 mild steel. From the above two cases it is very clear that the weld interface on the 2062 mild steel is the highest risk zone, where the failure is most likely to occur[3]. The shear stress distribution along the line P is shown in Fig. 10. The value of von-mises stresses developed in the welded joint in the model is 306 MPa of the tensile nature and 169 MPa of the compressive nature. The maximum tensile stress is located at the center of the welded joint and is much localized as shown in Fig. 11. The total deformation result shows that tensile value in the weld joint to be 410 MPa then the weld zone to be deformed. The total stress occurred in the center line of the weld joint (fig 11 and 12). In line with the stresses the contour of equivalent strain also depicts that a maximum strain of 0.001 m/m is also located in the weld interface on the IS 2062 mild steel side. This means that this interface has the highest deformation.

4. CONCLUSION

In this Experimental work presents a study of mechanical properties in a dissimilar welding joint between IS 2062GrC mild steel and AISI 316L stainless steel, using AISI 309L filler rod. It increases the weld zone strength has been discussed. The hardness survey revealed that weld zone hardness is increased as a result of base metal dilution. In addition, the HAZ of solutionized 316L will increase in strength. The weld tensile test indicated that a AISI 316L and IS 2062C dissimilar metal with AISI 309L as filler using GTAW process can be performed as a strength of 394 to 454 MPa, whereas yield strength of MS is about 200Mpa. It indicates it would increase the total yield strength of specimen. Microstructure analysis shows the change of metal migration towards base metal .On studying fusion zone and HAZ of mild steel and stainless steel on using AISI 309L have higher dilution of base metals in weld area. Hence, the welded area strength is better. The welding responses like depth of penetration, weld bead width were observed to be sufficient enough to make perfect welding in single pass as welding of 6 mm thick plate it was penetration more than 5.5 mm

REFERENCES

1. Chengwu Yao, Binshi Xu, Xiancheng Zhang, Jian, Huang, Jun Fu and Yixiong Wu "Interface microstructure and mechanical properties of laser welding copper-steel dissimilar joint" Optics and Lasers in Engineering, Vol. 47, 2016, PP 807–814.

2. Wen-chun Jiang and Xue-wei Guan "A study of the residual stress and deformation in the welding between half-pipe jacket and shell" Materials and Design, Vol. 43, 2013, PP 213-219.

3. Man Gyun Na, Jin Weon Kim and Dong Hyuk Lim "Prediction of Residual Stress for dissimilar metals welding at nuclear plants using Fuzzy Neural Network Models" Nuclear Engineering and Technology, Vol. 39, 2017, PP 337-348.

4. M.M.A. Khan, L. Romoli, M. Fiaschi, G. Dini and F. Sarri "Laser beam welding of dissimilar stainless steels in a fillet joint configuration" Journal of Materials Processing Technology, Vol. 212, 2012, PP 856-867.

5. Yoshiyasu Itoh and Kabushiki Kaisha Toshiba "Joined structure of dissimilar metallic materials" Patent Publication Number, EP0923145A2, 2015.

6. P. Delphin, I. Sattari-Far and B. Brickstad "Effect of thermal and weld induced residual stresses on the j-integral and ctod in elastic-plastic fracture analyses" Final Report Vol. SINTAP/SAQ/03, 1998, PP 1-47.

7. T.A. Mai and A.C. Spowage "Characterization of dissimilar joints in laser welding of steel-kovar, copper-steel and copper-aluminium" Materials Science and Engineering, Vol. 374, 2014, PP 224-233.

8. Paul Colegrove, Chukwugozie Ikeagu, Adam Thistlethwaite, Stewart Williams, Tamas Nagy, Wojciech Suder, Axel Steuwer and Thilo Pirling " The welding process impact on residual stress and distortion" Science and Technology of Welding and Joining, Vol. 14, 2015, PP 717-725.

9. N. Arunkumar, P. Duraisamy and S. Veeramanikandan "Evaluation Of Mechanical Properties Of Dissimilar Metal Tube Welded Joints Using Inert Gas Welding" International Journal of Engineering Research and Applications, Vol. 2, Issue 5, 2012, PP 1709-1717.

10. Subodh Kumar, A.S. Shahi,(2011) "Effect of heat input on the microstructure and mechanical properties of gas tungsten arc welded AISI 304 stainless steel joints", material and design, v. 6, pp. 3617–3623.

11. Shaohua Yana, Yuan Niea, Zongtao Zhua, Hui Chena, Guoqing Goua, Jinpeng Yub, GuiguoWangb (2014). "Characteristics of microstructure and fatigue resistance of hybrid fiber laser-MIG welded Al–Mg alloy joints"' Applied Surface Science, v.298, pp. 12-18.

12. Jun Yan, Ming Gao, Xiaoyan Zeng (2009), "Study on microstructure and mechanical properties of 304 stainless steel joints by TIG, laser and laser-TIG hybrid welding", Optics and Lasers in Engineering, v.48, pp. 512-517.